Concept and Performance of Internal Instrument Calibration for Multi-Channel SAR

Marwan Younis[(1)], Christopher Laux[(1)], Andrea Loinger[(2)], Grzegorz Adamiuk[(2)], Michael Ludwig[(3)], Dirk Geudtner[(3)], Gerhard Krieger[(1)]

[(1)] Microwaves and Radar Institute, German Aerospace Center (DLR), Germany
[(2)] Airbus Defense and Space GmbH, Space Systems, Germany
[(3)] European Space Agency, ESA/ESTEC, The Netherlands

Abstract

The increased complexity of multi-channel SAR sensors and the real-time on-board phase/amplitude correction requirement poses new challenges for the calibration, which cannot rely on current calibration techniques. On the other hand, the digital hardware utilized in multi-channel SAR systems, offer entirely new opportunities for the calibration such as on-board error correction and digital calibration. An internal calibration strategy for future digital beamforming SAR instruments is detailed and its performance analyzed using a dedicated calibration simulator software.

1 Baseline Instrument

A multi-channel SAR instrument utilizing digital beam-forming similar to the Sentinel-1 Next Generation instruments [5,6] is considered here. The planar direct radiating SAR antenna consists of multiple antenna elements in along-track (azimuth) and across-track (elevation) direction, where each antenna element is equipped with Transmit/Receive Modules (TRM).

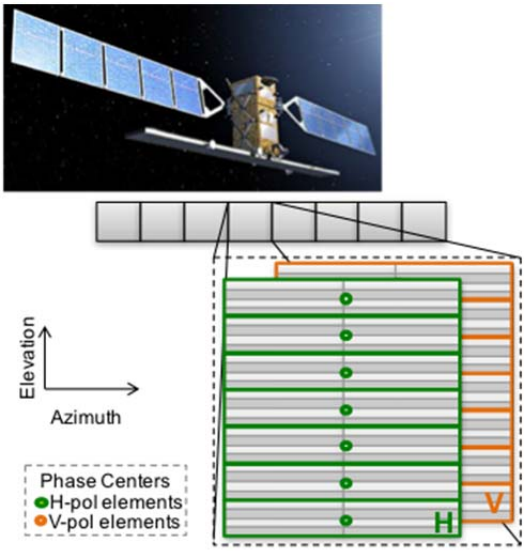

Figure 1: Sentinel-1 Next Generation system concept.

On-transmit, phase spoiling is applied to get an antenna beam wider than what would normally be the case for a large antenna; this is because all the TRMs are active, i.e. transmitting. The reflected echo signal is received by the antenna elements, amplified, partially combined with the signals of other elements, and the resulting signals filtered, down-converted and digitized. This forms *Naz*×*Nel* azimuth and elevation data streams, respectively. First, digital beam-forming is applied on-board through Scan-On-REceive (SCORE) in elevation. Second, MACS (Multiple Azimuth Channels) requires reconstructing the Doppler spectrum from the undersampled azimuth channels data, which is applied on-ground.

2 Calibration Concept

The instrument calibration has two particularities when compared to conventional instrument calibration: a CW signal is injected (instead of the typically used chirp) and the raw received SAR data are used for calibration. Each of these are explained in the following. Combined, these result in a hybrid instrument calibration mode.

2.1 Cal-Tone Injection

The main characteristic of the suggested calibration concept is that it avoids the typical interruption of SAR operation when injecting the calibration signal –which would cause lost imaging pulses or a reduction in swath width–, and that it allows for on-board channel correction. This is done through single tone (i.e. single frequency) signals outside the SAR signals chirp bandwidth, which can be injected together with the chirp and echo signal without disturbing SAR operation similar to the approach in [2]. Using these single tone calibration signals the calibration methodology for the instrument including the front-end TRMs, the radio frequency unit (RFU), the digital beamforming unit (DBFU), and the CE is possible [9]. **Figure 2** shows the injection point and path of the cal-tone in the TRM. It should be noted that the calibration concept is of limited sensitivity to variations within the chirp bandwidth, but

is considered sufficient given the typical SAR instrument transfer functions [6]; also the cal-tone frequency can even be placed within the chirp bandwidth, as it can be removed in the DBU.

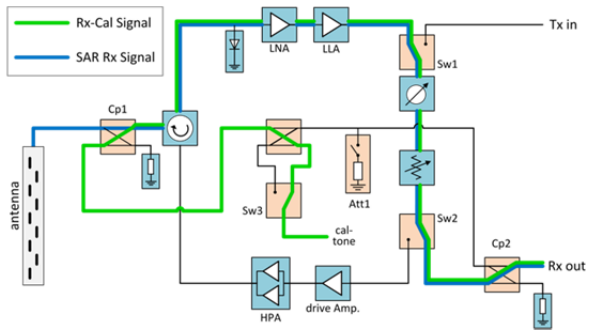

Figure 2: Transmit/Receive Module (TRM) topology showing the SAR receive and Rx-Cal signal paths.

Advantages of the calibration concept are: it simplifies the TRM design and increases reliability by reducing the number of switches in the signal path; it allows for simultaneous SAR operation and calibration, i.e. uninterrupted SAR operation; and the concept makes extensive use of the on-board digital processing capabilities to measure and correct the instrument drifts in real time.

2.2 Raw Data-Based Calibration

Internal instrument calibration schemes, such as the one above, that rely on injecting calibration signals into the transmitter and/or receiver path are inherently incapable of measuring contributions beyond the injection point (typically a coupler). These error contributions, which mainly include the RF cabling to the antenna and the antenna itself, are thus not measured and remain unknown. In addition to this, the calibration signal levels at the input of the digitizers (analog-to-digital converters) may be different from those of the SAR signals, and thus not representative for the actual signal path. Most state-of-the-art internal SAR calibration concepts rely on calibration signals.

These and other deficiencies addressed in [1] are overcome by using data driven calibration, meaning that the channel errors are extracted (measured) from the raw received SAR data. Data driven calibration algorithms are typically based on the correlation between the receive signals of different channels and some metric to extract the errors. For example, the method in [4] shows that the correlation between the signals of any two antenna elements (spatial correlation) depends only on the separation between the two elements (as shown in **Figure 3**). The underlying model assumes the signals to originate from non-coherent scatterers, i.e. the typical raw echo signal (clutter) of a radar imaging a distributed homogeneous scene. Other algorithms are available in the literature, such as [3] which uses an approach based on maximizing the contrast, which may be applied to heterogeneous scenes.

A particularity of data driven calibration is, that it is not suitable for transmit path characterization[1]. On the other hand, only passive and thus reciprocal RF hardware contributes to drifts beyond the coupler; these contributions are captured on-receive by the data driven calibration and can thus be removed.

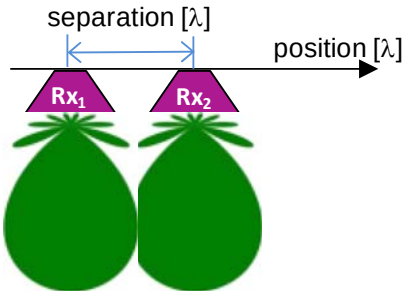

Figure 3: In the clutter raw data calibration it is shown that the signals received by any two antenna elements are statistically determined solemnly by the separation of the antenna elements.

Moreover, most data driven calibration techniques are suitable for correcting slowly varying errors. This is because of the computational load and the number of independent measurements needed. This is also true for the technique described here, which is understood to compensate/correct slow instrument drifts.

Raw data based techniques are especially suitable for real-time calibration of the time varying beams used in the Scan-On-REceive (SCORE) mode of operation; this is because the small separation between the elevation channels guarantees a high degree of correlation between the channels, and because the algorithms can be implemented on the same digital hardware utilized for the SCORE digital beamforming.

3 Instrument Simulator Software

To assess the impact of instruments errors on the performance, and to evaluate the quality of the calibration concepts a calibration simulator is implemented. The implementation models the instrument hardware including its imperfections affecting the SAR signals in addition to the calibration sequence itself and the algorithms used to extract the correction factors.

The aim is to estimate the effect of the instrument's imperfections on the final SAR performance. For some special cases this can be determined analytically [7,8]. However, specifically in the case of an real-time on-board calibration the processes are no longer stationary and the assessment of the residual error is better done using simulations.

[1] Some calibration schemes re-inject the Tx signal into the Rx path, which would thus technically allow the use of data driven calibration.

In the following a generic receive hardware topology is used to explain the approach of the simulator software. Then various instrument error sources are introduced and shown.

3.1 Software Implementation of Hardware Model and Topology

The instrument schematic for one azimuth channel of the baseline system is shown in **Figure 4** focusing on the receive case, i.e. the transmit paths are not shown. Starting from the left, the reflected radar echo excites the antenna elements and the received signals are then passed through the TRMs for amplification and possible phase/amplitude setting. The signals comprising one elevation channels are combined in the Radio Frequency Units, thus *Nel* RFUs per azimuth channel and polarization are used, where the signals are further amplified, filtered, and down converted to IF. The output signal of each RFU is then digitized in the Digital Beamforming Unit which also applies the digital time varying weights necessary for SCORE operation. The output signals of each DBU are, however, analog (see DAC within DBU) which are then combined and, again, digitized within the CE so that it can be stored in the SSMM.

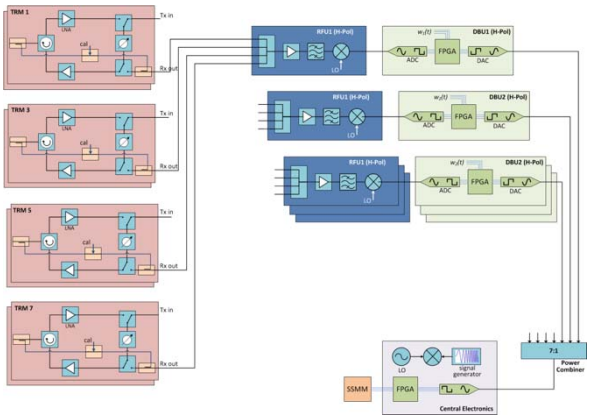

Figure 4: Instrument schematic used as the basis for implementing the calibration simulation software. Here, only the receive signal path of a single azimuth channel is shown.

The software is implemented in a generic object-oriented manner. Thus, first the receive signal path is sub-divided into layers such that each layer contains one or more similar components (or sub-units), which are described through classes. Each component may have individual parameters set during the initialization of the objects instance. **Figure 5** shows examples of classes for various sub-units and the parameters describing its properties. For example an ADC may be described through its number of bits and the clipping voltage. The components affect the signals passing through it, which is modelled as methods of the class. In the case of cables (harness class) this is straight forward, as each class has only one method. For the case of the TRMs this is more complicated as one and the same TRM has different paths for the transmit, receive, and calibration signals. A temperature drift of the TRM will affect all paths, although each path introduces individual errors.

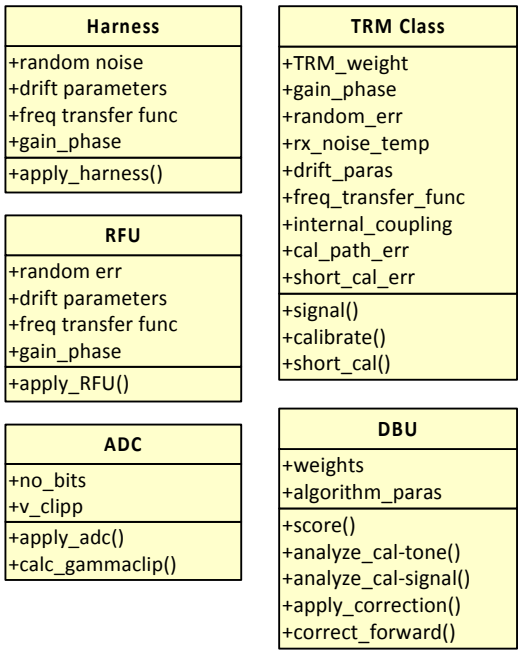

Figure 5: Modelling the hardware sub-units through object oriented classes.

As such, the effect the components/sub-units of each layer on the signal passing through it can be modelled. To take the actual instrument topology into account it is necessary to introduce a description how the components of different layers are connected to each other. This is done through pointer cells: each components instance has a numbered cell, the cells of components of the same layer are numbered sequentially. Each cell contains itself a pointer to one cell of a component of the previous layer. For example, a 4:1 combiner (components) will have a single pointer cell numbered 1; while the pointer cell of each of the cable instances contain a 1 indicating that the output signal of the cable is summed in the combiner. **Figure 6** shows example of the pointer cell structure of various layers.

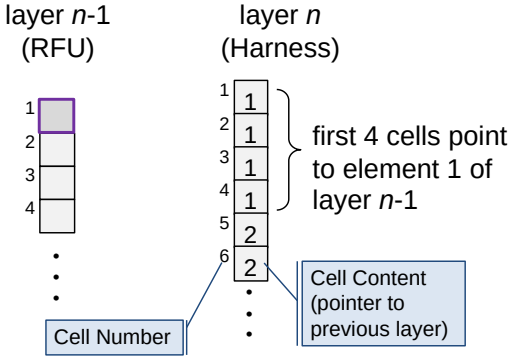

Figure 6: Pointer cells describing the instrument topology, i.e. components interconnections.

3.2 Phase and Amplitude Error Sources

Various error sources are implemented in the software starting from simple linear amplitude/phase drifts (cf. **Figure 7** top) which may occur for example in cables due to temperature variations and are modelled as

$$d_{lin}(t) = (\tau_a t + 1)e^{-j\tau_p t}$$

where t is the time, while τ_a and τ_p the amplitude and phase drift rates, respectively.

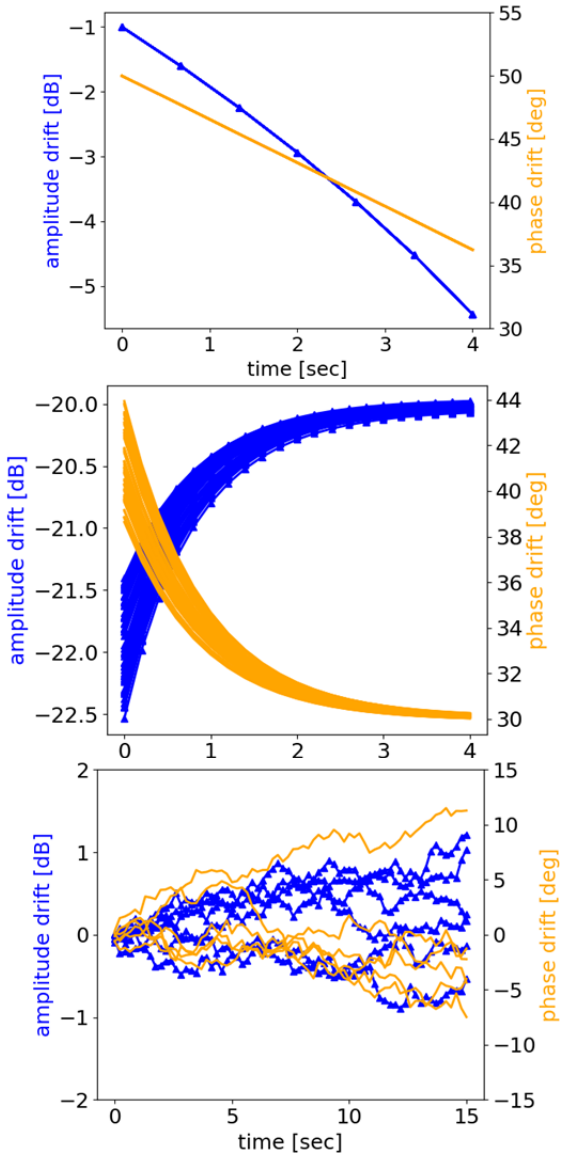

Figure 7: Examples of linear (top) and exponential (mid) and random walk (bottom) drift versus time affecting the amplitude and phase drift of the signal.

More elaborate drift models include exponential and random walk drift, the latter occurs for example in TRMs as observed from in-orbit measurements of TerraSAR-X instrument. **Figure 7** middle shows the simulated drift of the sub-units of one layer; notice that although all components are affected by an exponential drift, however the drift parameters of the individual components might differ resulting in slightly different curves.

Other error sources are the receiver (thermal) noise which is modelled as complex additive Gaußian noise:

$$n(t) = n_I(t)\sqrt{\frac{\sigma_n}{2}} + n_Q(t)\sqrt{\frac{\sigma_n}{2}}$$

where σ_n^2 is the noise variance (power) and $n_I(t), n_Q(t)$ are the I and Q random components $\mathcal{N}(0,1)$.

Depending on the system bandwidth the signal spectrum may well be affected by the components of the system. This may also be considered as an unwanted spectrum modulation, specifically if the shape of the frequency transfer function changes due to temperature drifts or other effects. The effect of a transfer function is shown in **Figure 8**, the original (ideal) signal spectrum is square shaped (green curve), whereas the orange curve shows the amplitude of the transfer function. The signal spectrum (blue curves) is further effected by a drift and receiver noise.

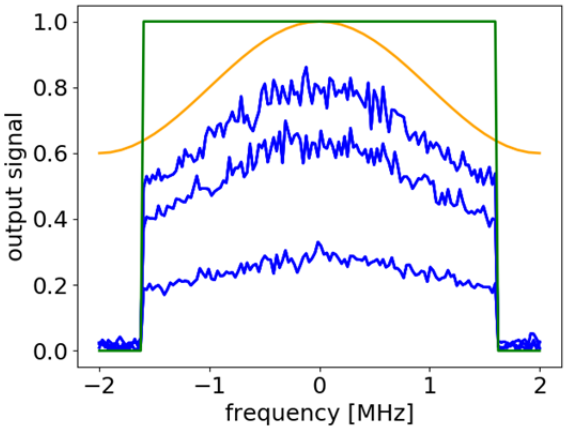

Figure 8: Example spectrum re-shaping due to the frequency transfer function of the instrument. The green curve shows the assumed original signal spectrum, while the orange curve represents the transfer function. The blue curves show the signal spectrum at various time instances which are affected by receiver noise and a drift.

A factor which may significantly affect the calibration accuracy itself is the coupling or bleed through. For the hybrid calibration scheme, this is mainly relevant for the Tx-Cal (cv. **Figure 2**) as the cal-tone has a dedicated injection point. Bleed through is modeled by adding an attenuated and phase shifted version of the signal to itself:

$$d_{coup} = 1 + \gamma e^{j\xi}$$

where γ is the coupling coefficient and ξ is the phase. The coupling effect is also implemented in the simulation software.

The resulting amplitude and phase error strongly depends on the (unknown) phase ξ. **Figure 9** shows the respective amplitude and phase errors versus the coupling coefficient. For example, requiring a gain error

of less than 1dB results in a coupling of less than -20dB, while a coupling factor of γ = -30dB results in a phase error of 2°.

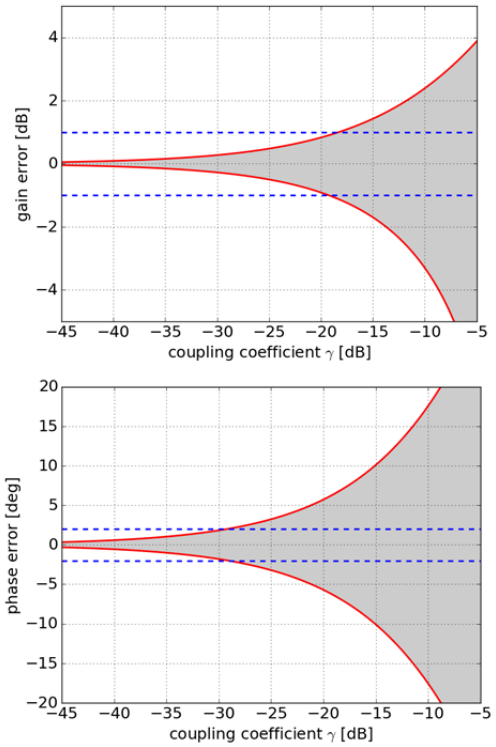

Figure 9: Amplitude (top) and phase (bottom) errors caused by a bleed-through (coupling) of the signal to the calibration path. The actual error depends on the phase of the coupled signal as represented by the gray area, whereas the red curves represent the respective maximum and minimum values.

4 Acknowledgement

The work is carried out jointly by DLR and Airbus DS under a contract with the European Space Agency (ESA/ESTEC) ESA ITT AO/1-8469/15/NL/FE

References

[1] M. Younis, C. Laux, N. Al-Kahachi, P. López-Dekker, G. Krieger, and A. Moreira, “Calibration of Multi-Channel Spaceborne SAR – Challenges and Strategies”, *proceedings European Conference on Synthetic Aperture Radar* (EUSAR'2014), Nuremberg, Germany, June 2014.

[2] J. Hoffman, S. Horst, L. Veilleux, H. Ghaemi, and S. Shaffer, “Digital calibration system enabling real-time on-orbit beamforming”, *proceedings IEEE Aerospace Conference*, March 2014.

[3] G. Farquharson, P. López-Dekker, and S. Fraiser, “Contrast-Based Phase Calibration for Remote Sensing Systems with Digital Beamforming Antennas”, in *IEEE Transactions on Geoscience and Remote Sensing*, vol. 51, no. 3, March 2013.

[4] E. Attia and B. Steinberg, “Self-cohering Large Antenna Arrays Using the Spatial Correlation Properties of Radar Clutter”, in *IEEE Transactions on Antennas and Propagation*, vol. 37, no. 1, January 1989.

[5] G. Adamiuk, C. Heer, and M. Ludwig, “DBF technology development for next generation of ESA C-Band SAR mission,” in Proc. European Conference on Synthetic Aperture Radar EUSAR’2016, Hamburg, Germany, June 2016.

[6] “Calibration and data reduction for digital beam forming instruments – concept discussion,” European Space Agency (ESA/ESTEC), technical report D1, ESA ITT AO/1-8469/15/NL/FE, Mar. 2017.

[7] E. Makhoul, A. Broquetas, P. López-Dekker, J. Closa, and P. Saameno, "Evaluation of the Internal Calibration Methodologies for Spaceborne Synthetic Aperture Radar with Active Phased Array Antennas", *IEEE Journal on Selected Topics in Applied Earth Observation and Remote Sensing*, vol. 5, issue 3, June 2012.

[8] F. de Almeida, M. Younis, G. Krieger and A. Moreira, "An Analytical Error Model for Spaceborne SAR Multichannel Azimuth Reconstruction”, *IEEE Geoscience and Remote Sensing Letters*, published, March 2018.

[9] M. Younis, T. Rommel, F. de Almeida, S. Huber, M. Martone, V. Villano, and G. Krieger, "Investigations on the internal calibration of multi-channel SAR," in *IEEE International Geoscience and Remote Sensing Symposium* (IGARSS), Fort Worth, USA, 2017, pp. 5386-5389